

Evidence for Thermal Equilibration in Multifragmentation Reactions probed with Bremsstrahlung Photons

D.G. d'Enterria,^{1,5,*} L. Aphecetche,^{1,*} A. Chbihi,¹ H. Delagrange,^{1,*} J. Díaz,² M.J. van Goethem,^{3,†} M. Hoefman,³ A. Kugler,⁴ H. Löhner,³ G. Martínez,^{1,*} M.J. Mora,^{1,*} R. Ortega,⁵ R. Ostendorf,³ S. Schadmand,⁶ Y. Schutz,^{1,*} R.H. Siemssen,³ D. Stracener,⁷ P. Tlusty,⁴ R. Turrisi,^{1,‡} M. Volkerts,³ V. Wagner,⁴ H. Wilschut,³ and N. Yahlali²

¹*Grand Accélérateur National d'Ions Lourds, BP 5027, 14076 Caen Cedex 5, France*

²*Institut de Física Corpuscular, Universitat de València-CSIC, Dr. Moliner 50, 46100 Burjassot, Spain*

³*Kernfysisch Versneller Instituut, 9747 AA Groningen, The Netherlands*

⁴*Institute of Nuclear Physics, 25068 Řež, Czech Republic*

⁵*Grup de Física de les Radiacions, Universitat Autònoma de Barcelona, 08193 Cerdanyola del Vallès, Catalonia*

⁶*II. Physikalisches Institut, Universität Gießen, D-35392 Gießen, Germany*

⁷*Oak Ridge National Laboratory, Oak Ridge, Tennessee 37831*

(November 3, 2018)

The production of nuclear bremsstrahlung photons ($E_\gamma > 30$ MeV) has been studied in inclusive and exclusive measurements in four heavy-ion reactions at 60A MeV. The measured photon spectra, angular distributions and multiplicities indicate that a significant part of the hard-photons are emitted in secondary nucleon-nucleon collisions from a thermally equilibrated system. The observation of the thermal component in multi-fragment $^{36}\text{Ar}+^{197}\text{Au}$ reactions suggests that the breakup of the thermalized source produced in this system occurs on a rather long time-scale.

21.65.+f, 25.70.-z, 25.70.Pq, 24.30.Cz

Nucleus-nucleus collisions at intermediate energies ($20A \text{ MeV} \leq \epsilon_{lab} \leq 100A \text{ MeV}$) aim at the study of the phase diagram of nuclear matter at densities and temperatures where a transition from the Fermi liquid ground-state to the nucleon gas phase has been predicted [1]. The experimentally observed production of several intermediate-mass fragments, IMF, with $3 \leq Z \leq 20$ (“nuclear multifragmentation”) has usually been interpreted as a signal of such a liquid-gas phase transition [1,2]. One of the key issues in the field is whether or not an equilibrated system is created in the course of the collision [3,4] and, implicitly, whether its lifetime is long enough for equilibration to occur. Despite their low production rates, “elementary” particles such as photons, dileptons and mesons, are unique probes of the phase-space evolution of nucleus-nucleus collisions [5]. At variance with charged particles and nuclear fragments, photons are primordial observables because they do not suffer final-state (neither Coulomb nor strong) interactions with the surrounding medium, thus providing an unperturbed image of the emission source. Above $E_\gamma = 30$ MeV, many experimental facts supported by model calculations [5–7] indicate that photons are mainly emitted during the first instants of the reaction in incoherent proton-neutron bremsstrahlung collisions, $pn \rightarrow pn\gamma$, occurring within the participant zone. Hard-photons have thus been exploited to probe the preequilibrium conditions prevailing in the initial high-density phase of the reaction [7,8]. Recent experimental results have pointed out an additional source of hard-photon emission, softer than the one originating in first-chance $pn\gamma$, accounting for up to a third of the total hard-photon yield [9,10].

The origin of this second component has been localized in secondary $NN\gamma$ collisions within a thermalizing system [7,9,10]. Such thermal hard-photons hence constitute a novel and clean probe of the intermediate dissipative stages of the reaction where nuclear fragmentation is supposed to take place, characterizing both its time-scale and the thermodynamical state of the fragmenting source(s). This information is essential to establish whether the physical mechanism driving multifragmentation is of fast statistical [11,12], sequential [13] or purely dynamical [14] origin. In this Letter, we first establish the thermal origin of second-chance hard-photons from inclusive measurements in four heavy-ion reactions at 60A MeV. Additionally, the concomitant observation of thermal hard-photon and IMF emission in the $^{36}\text{Ar}+^{197}\text{Au}$ system indicates that multifragmentation is, at least for this reaction, a slow process preceded by the thermalization of the system.

The inclusive and exclusive hard-photon and fragment production in $^{36}\text{Ar}+^{197}\text{Au}$ at 60A MeV, and the inclusive hard-photon production in the $^{36}\text{Ar}+^{107}\text{Ag}$, ^{58}Ni , ^{12}C reactions at 60A MeV have been studied at the KVI laboratory. The ^{36}Ar beam was delivered by the $K = 600$ MeV superconducting AGOR cyclotron with a bunch rate of 37.1 MHz and with intensities ranging from 3.0 to 12.5 nA. Targets consisted of thin isotopically enriched foils of 1 to 18 mg/cm². The TAPS [15] electromagnetic spectrometer, comprising 384 BaF₂ scintillation modules in a six-block configuration and covering the polar angles between 57° and 176° and the azimuthal range from -20° to 20°, was used to measure the double differential cross section $d^2\sigma/d\Omega_\gamma dE_\gamma$ for photons of 10

MeV $\leq E_\gamma \leq 300$ MeV. Photons have been discriminated against charged particles and neutrons on the basis of pulse-shape analysis, time-of-flight and charged-particle veto information [16,17]. Two phoswich multidetectors, the Washington University “Dwarf-Ball” (DB) [18] and the KVI “Forward Wall” (FW) [19], were added to TAPS to allow the isotopic identification of the light charged particles (LCP: p , d , t , ${}^3\text{He}$ and α) and the charge of the IMFs up to that of the projectile by means of pulse-shape techniques. The DB was composed of 64 BC400-CsI(Tl) phoswich telescopes in the angular range $32^\circ < \theta < 168^\circ$ covering about 76% of 4π , and the FW hodoscope comprised 92 NE102A-NE115 ΔE -E phoswich detectors in the forward region ($2.5^\circ < \theta < 25^\circ$). Altogether, more than $1.2 \cdot 10^6$ hard-photons were collected in the four reactions with a trigger defined by at least one neutral hit in TAPS depositing more than 10 MeV in a single BaF₂ crystal, plus three or more hits in the charged particle detectors. The inclusive photon energy spectra have been obtained after correction for the detector response and after subtraction of the cosmic and π^0 -decay (measured via $\gamma\gamma$ invariant mass analysis) backgrounds which amount to $(5 \pm 1)\%$ of the total yield [17]. The hard-photon spectra of the Au, Ag and Ni targets feature two distinct components above 30 MeV (Fig. 1 left, for the Au target) and can be described by the sum of two exponential distributions characterized by inverse slopes E_0^d and E_0^t , corresponding to a “direct” (first-chance) and a “thermal” (secondary $pn\gamma$) component, with their corresponding weights [7,9]:

$$\frac{d\sigma}{dE_\gamma} = K_d e^{-E_\gamma/E_0^d} + K_t e^{-E_\gamma/E_0^t} \quad (1)$$

The direct slopes of the three heaviest targets, $E_0^d \approx 20$ MeV, are two to three times larger than the thermal ones, $E_0^t \approx 6 - 9$ MeV, and the thermal contribution represents 15% - 20% of the total yield (Table I). No thermal component is apparent in the photon spectrum measured in the ${}^{36}\text{Ar}+{}^{12}\text{C}$ reaction and direct bremsstrahlung alone accounts for the whole photon emission already above $E_\gamma \approx 20$ MeV (Fig. 1, right). As a matter of fact, in such a light system there are not enough nucleons in the overlap volume of target and projectile to experience more than the minimal 2-3 collisions needed for thermalization to take place (the average number of pn collisions in this system is $\langle N_{pn} \rangle = 1.8$ according to the “equal-participant” geometrical model [6]). Since no sufficient stopping and equilibration are achieved, pure first-chance bremsstrahlung dominates the entire hard-photon emission. Direct slopes, independently of the system size, are proportional to the laboratory projectile energy per nucleon, ϵ_{lab} , as expected for pre-equilibrium emission in prompt NN collisions and in good agreement with the systematics [7]. This dependence does not apply to thermal hard-photons: their slopes scale with the total

energy available in the nucleus-nucleus center-of-mass, ϵ_{AA} (Fig. 2), strongly supporting the fact that thermal hard-photons originate at later stages of the reaction after dissipation of the incident energy into internal degrees of freedom over the whole system in the AA center-of-mass. The thermal slopes, lower by a factor two to three than the direct ones, reflect the lesser energy available in secondary NN collisions.

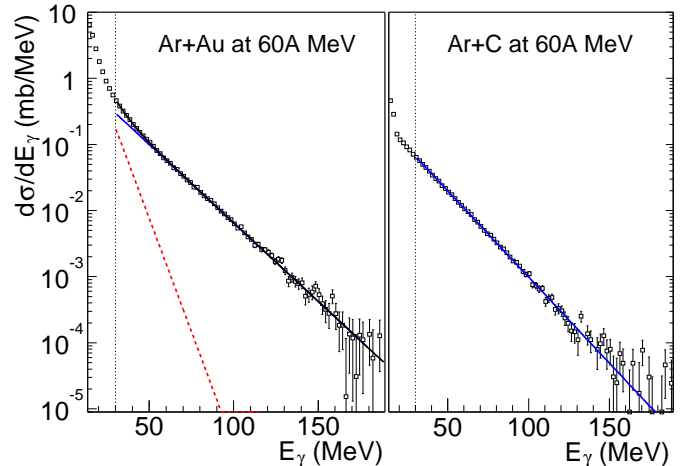


FIG. 1. Hard-photon ($E_\gamma > 30$ MeV) spectra for: ${}^{36}\text{Ar}+{}^{197}\text{Au}$ (left), fitted to the sum of a direct (solid) and a thermal (dashed) exponential distribution; and ${}^{36}\text{Ar}+{}^{12}\text{C}$ (right) fitted to a single exponential.

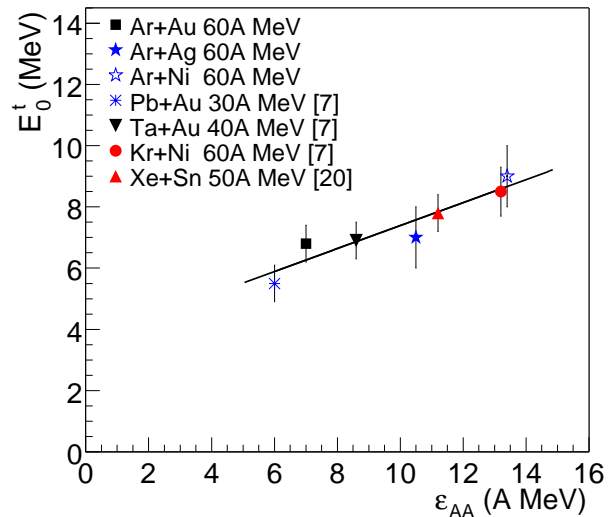


FIG. 2. Thermal hard-photon slopes E_0^t (measured at $\theta_{lab}=90^\circ$) as a function of the (Coulomb-corrected) nucleus-nucleus center-of-mass energy, ϵ_{AA} , for the 7 reactions studied by TAPS: the 3 heavy systems reported here, and those of refs. [7,20]. The solid line is a linear fit to the data.

TABLE I. Direct and thermal slopes (inclusive, and at $\theta_{lab}=90^\circ \pm 2^\circ$ to minimize Doppler effects), ratios of thermal to total intensities, source velocities of both components, and total cross-sections, for the hard-photons measured in $^{36}\text{Ar}+^{197}\text{Au}$ (inclusive, multifragment and central reactions), ^{107}Ag , ^{58}Ni , ^{12}C at 60A MeV. The errors include statistical and systematic effects. nss : not statistically significant.

System	E_0^d (MeV)	E_0^t (MeV)	$E_0^{t(90^\circ)}$ (MeV)	I_t/I_{tot} (%)	β_S^d	β_S^t/β_{AA}	$\sigma_{hard-\gamma}$ (mb)
$^{36}\text{Ar}+^{197}\text{Au}$	20.2 ± 1.2	6.2 ± 0.5	6.8 ± 0.6	19 ± 1	0.17 ± 0.02	1.6 ± 0.3	3.8 ± 0.2
$^{36}\text{Ar}+^{107}\text{Ag}$	20.1 ± 1.3	6.1 ± 0.6	7.0 ± 1.0	15 ± 1	0.18 ± 0.02	1.0 ± 0.3	3.1 ± 0.2
$^{36}\text{Ar}+^{58}\text{Ni}$	20.9 ± 1.3	8.8 ± 0.8	9.0 ± 1.0	20 ± 1	0.18 ± 0.03	1.4 ± 0.3	1.8 ± 0.1
$^{36}\text{Ar}+^{12}\text{C}$	18.1 ± 1.1	0.0 ± 0.5	0.0 ± 0.5	0 ± 2	0.20 ± 0.01	-	0.6 ± 0.1
$^{36}\text{Ar}+^{197}\text{Au}$ (multif.)	20.2 ± 1.3	6.0 ± 0.8	nss	16 ± 2	nss	nss	0.4 ± 0.1
$^{36}\text{Ar}+^{197}\text{Au}$ (central)	19.7 ± 1.3	6.2 ± 0.8	nss	18 ± 2	nss	nss	0.4 ± 0.1

The thermal origin of the second hard-photon component is confirmed by the analysis of the (Doppler-shifted) laboratory angular distributions. The hard-photon angular distributions of the three heaviest systems yield a source velocity which is systematically lower (by a factor 15%) than the NN center-of-mass velocity, β_{NN} , when assuming that they are emitted from a single moving source [17,21]. They can be well described, however, considering a midrapidity emission ($\beta_S^d \approx \beta_{NN} \approx 0.18$) with slope E_0^d plus an isotropic emission with slope E_0^t from a source moving with a reduced velocity close to the AA center-of-mass, β_{AA} , of each system (Table I). The ratios of thermal to direct intensities are fixed, in this double-source analysis, by the ratios measured in the energy spectra. All other potentially conceivable mechanisms for photon production above $E_\gamma = 30$ MeV (e.g. statistical photons from the high energy tail of Giant-Dipole Resonance (GDR) decays, coherent nucleus-nucleus, cluster-nucleus or $pp\gamma$ bremsstrahlung) investigated elsewhere [17], cannot consistently explain the full set of data.

The photon yield per nuclear reaction has been studied as a function of impact parameter in the $^{36}\text{Ar}+^{197}\text{Au}$ system using the charged-particle multiplicity, M_{cp} , measured by the phoswich multidetectors. We have classified the photons detected in TAPS into three broad categories: (1) statistical nuclear decay photons, with $E_\gamma = 10 - 18$ MeV, (2) thermal bremsstrahlung photons, in the range $E_\gamma = 25 - 35$ MeV, and (3) direct bremsstrahlung photons with $E_\gamma > 50$ MeV. Thermal and direct hard-photon multiplicities exhibit a very similar dependence with charged-particle multiplicity (Fig. 3), increasing by a factor ~ 10 from $M_{cp} = 2$ (peripheral) to $M_{cp} = 9$ (semi-central collisions). They stay roughly constant at $M_\gamma \approx 1.2 \cdot 10^{-3}$ for $M_{cp} = 9 - 18$ (semi-central and central reactions). This last class of events includes the reactions for which the incident ^{36}Ar is overlapped entirely by the much larger ^{197}Au target nucleus. Within this region of impact parameters, the number of NN collisions saturates and so does bremsstrahlung photon production. On the contrary, the statistical low-energy photon yield decreases for increasingly central reactions by a factor ~ 2 from $M_{cp} = 7$ to $M_{cp} \approx 20$. This result is consistent with

the quench of the GDR photon yield (the dominant component in the region $E_\gamma = 10 - 18$ MeV [22]) observed at high excitation energies [22,23] and interpreted as a result of the loss of collectivity due to a change from ordered mean-field-driven motion to chaotic nucleonic motion.

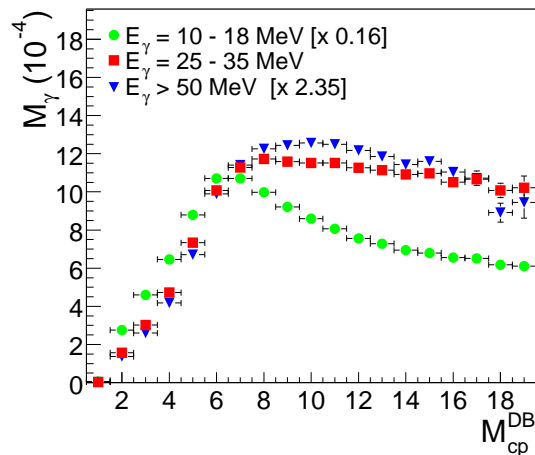


FIG. 3. Photon multiplicity, M_γ , as a function of the “Dwarf-Ball” charged-particle multiplicity, M_{cp}^{DB} , for: statistical nuclear photons (circles), thermal (squares) and direct hard-photons (triangles), emitted in $^{36}\text{Ar}+^{197}\text{Au}$ at 60A MeV. $M_\gamma[10-18$ MeV] and $M_\gamma[>50$ MeV] have been scaled to $M_\gamma[25-35$ MeV] (the scaling factor is given in brackets). The M_γ systematic errors (not shown) are below 10%.

Multi-fragment exit-channels, with $M_{IMF}^{DB} \geq 3$, account for 8% of the total $^{36}\text{Ar}+^{197}\text{Au}$ reaction cross-section. Interestingly, those reactions (as well as the 9% most central reactions with $M_{cp} > 15$) show also a thermal bremsstrahlung component with roughly the same slope and intensity as found in the inclusive case (Fig. 4 and Table I). The concurrent observation of IMF and thermal bremsstrahlung emission in Ar+Au sets a lower limit for the fragmentation time-scale. All microscopic transport models [3,5,14], in agreement with the available data [24], indicate that the primary mechanism in intermediate-energy heavy-ion reactions are quasi-binary dissipative processes in which two excited and expanding

quasi-target and quasi-projectile emerge right after having traversed each other. The transient time up to the moment when both ions loose contact is $t \approx 2R_A/\beta \approx 80 \pm 20$ fm/c, a time that characterizes the end of the pure pre-equilibrium phase [3]. If, as observed, thermal $NN\gamma$ collisions occur within the produced hot system, two conditions have to be met: i) equilibration has been previously reached, and ii) the radiating source has not yet fully fragmented. Microscopic calculations of the Boltzmann-equation [5] or molecular-dynamics [14] type for the $^{36}\text{Ar}+^{197}\text{Au}$ system [9,17] show that second-chance $NN\gamma$ collisions take place at $t \approx 100$ -200 fm/c during the first compression undergone by the heavy quasi-target when it reverts towards normal density after separating from the projectile. Thus, the source has to break-up at times, $t \gtrsim 150$ fm/c, more consistent with a “sequential” scenario [25], than with a fast ($t < 100$ fm/c) fragmentation in a more dilute state. The validity of such conclusions for central collisions of more symmetric systems is presently under study [20].

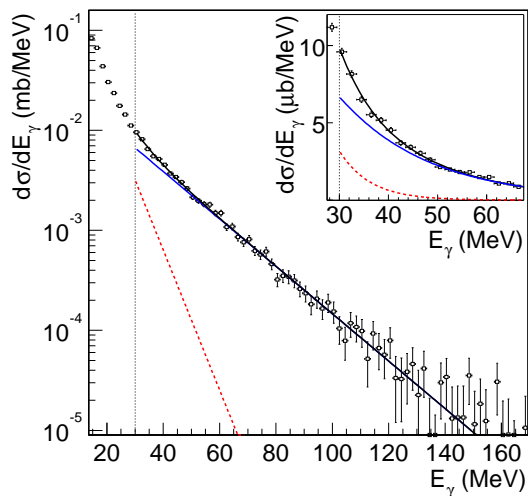


FIG. 4. Hard-photon ($E_\gamma > 30$ MeV) spectrum in $^{36}\text{Ar}+^{197}\text{Au}$ reactions with $M_{IMF}^{DB} \geq 3$, fitted to the sum of a direct (solid) and a thermal (dashed) exponential. The thermal component is more apparent on a linear scale in the inset.

In summary, hard-photon production has been investigated in four Ar-induced reactions at 60A MeV. Aside from the dominant emission in first-chance (off-equilibrium) $NN\gamma$ collisions, a second thermal bremsstrahlung component is observed. The thermal origin of these photons is inferred based on: i) their presence in the three heaviest systems, accounting for 15%-20% of the total hard-photon yield, and their absence in the light $^{36}\text{Ar}+^{12}\text{C}$ system which does not provide enough secondary collisions; ii) the scaling of the thermal slopes with the AA center-of-mass energy as expected for a process taking place after dissipation of the energy into internal degrees of freedom; iii) the consistency of

the source velocity analysis with a later isotropic emission for the thermal component; iv) the significantly different behaviour of statistical GDR photon and thermal hard-photon yields for increasing centrality suggesting a change from nuclear collective to nucleonic chaotic motion. The persistence of the thermal component in multifragment $^{36}\text{Ar}+^{197}\text{Au}$ reactions sets a longer time-scale for nuclear multifragmentation than expected from pure dynamical or simultaneous statistical models.

We thank the AGOR accelerator team for providing a high-quality beam. We gratefully acknowledge the loan of the “Dwarf-Ball” array and the support from W.U. Schroeder, L. Sobotka and J. Töke. This work has in part been supported by the IN2P3-CICYT agreement, the Stichting FOM, and by the European Union HCM network under Contract No. HRXCT94066.

-
- * Now at SUBATECH, BP 20722, 44307 Nantes, France.
 - † Now at NSCL, MSU, East Lansing, Michigan 48824-1321.
 - ‡ Now at INFN-Padova, V. Marzolo 8, 35131 Padova, Italy.
 - [1] J. Pochodzalla, *Prog. Part. Nucl. Phys.* **39**, 443 (1997).
 - [2] S. Das Gupta *et al.*, nucl-th/0009033.
 - [3] J. Richert and P. Wagner, nucl-th/0009023.
 - [4] “Multifragmentation”, *Proceed. Int. Workshop XXVII on Gross Prop. of Nuclei and Nuc. Excitations*, Hirscheegg, Austria, ed. H. Feldmeier *et al.*, GSI, Darmstadt, 1999.
 - [5] W. Cassing *et al.*, *Phys. Rep.* **188**, 363 (1990).
 - [6] H. Nifenecker and J. Pinston, *Ann. Rev. Nucl. Part. Sci.* **40**, 113 (1990).
 - [7] Y. Schutz *et al.*, *Nucl. Phys.* **A622**, 405 (1997).
 - [8] G. Martínez *et al.*, *Phys. Lett.* **B334**, 23 (1994).
 - [9] G. Martínez *et al.*, *Phys. Lett.* **B349**, 23 (1995).
 - [10] F.M. Marqués *et al.*, *Phys. Lett.* **B349**, 30 (1995).
 - [11] J.P. Bondorf *et al.*, *Phys. Rep.* **257**, 133 (1995).
 - [12] D.H. Gross, *Phys. Rep.* **279**, 119 (1997).
 - [13] W.A. Friedman, *Phys. Rev. C* **42**, 667 (1990).
 - [14] J. Aichelin, *Phys. Rep.* **202**, 233 (1991).
 - [15] R. Novotny, *IEEE Trans. Nucl. Sci.* **38**, 379 (1991).
 - [16] F.M. Marqués *et al.*, *Nucl. Inst. and Meth.* **A365**, 392 (1995).
 - [17] D.G. d’Enterria, PhD thesis, Univ. Autònoma Barcelona and Univ. Caen, May 2000.
 - [18] D. Stracener *et al.*, *Nucl. Inst. and Meth.* **A294**, 485 (1990).
 - [19] H. Leegte *et al.*, *Nucl. Inst. and Meth.* **A313**, 26 (1992).
 - [20] R. Ortega, *Czech. Jour. Phys.* **50** S4, 91 (1999).
 - [21] D.G. d’Enterria and G. Martínez, *Czech. Jour. Phys.* **50** S4, 103 (1999); nucl-ex/0007005.
 - [22] J.J. Gaardhoje, *Ann. Rev. Nucl. Part. Sci.* **42**, 483 (1992).
 - [23] T. Suomijärvi *et al.*, in *RIKEN Symposium on Dynamics in Hot Nuclei*, IPNO DRE 98-09.
 - [24] D. Durand, *Nucl. Phys.* **A654**, 273c (1999).
 - [25] W.A. Friedman, *Phys. Rev. C* **60**, 044603 (1999).